Imaged-Based PID Control of a Ping Pong Ball

Salvador Alvizar, Mark Ansell, Brian Lo, Lily Zheng

December 8, 2019

ABSTRACT

Current unmanned aerial vehicles (UAVs) use a variety of onboard sensors, including accelerometers, tilt sensors, and internal measurement units, in order to control their flight and vertical stabilization. These sensors can be costly, especially when flying multiple UAVs at a time, and there is a high risk of losing these components in the event of a crash. Therefore, the team proposes a propeller-actuated vertical stabilization mechanism using an image-based measurement input from an external camera driven to a PID controller. An imaging system is applied to the image from the camera to track the vertical location of the object. This location data is then input to the controller, which manipulates the voltage provided to the propeller/fan. This method was simulated through multiple tests of dropping a ping-pong ball, from out of view of a camera, into a tube with a fan located at the bottom of the tube. The results of this experiment reveal that position control using an image-based input can be accomplished in real time, though the biggest contributors to inefficient performance of the controller are camera and fan voltage calibration uncertainty. The effect of these sources of uncertainty may be able to be decreased by further tuning the PID controller gains. Taking into account the obstacles and limitations of using an image-based input to control the vertical location of a UAV demonstrated by the results of the experiment, the team believes that commanding the vertical location of a UAV using an image-based input is a viable option.

INTRODUCTION

The main question that our experiment is trying to solve is: can image-based measurements be used to inform a PID controller, connected to a fan, to command the vertical location of an aerial object, using the ball's center as the reference point? In many previous works, PID controllers have been used to levitate a ping pong ball from rest [2][1][6]; however, our experiment will test a PID controller's ability to decelerate a falling ping pong ball and bring it to rest at a desired height. Can this be done within a specified rise time, without significant overshoot, and without previous knowledge of the starting height? To answer the research question, the team dropped the ball from outside of the field of view of the camera from various heights (1.969in (5cm), 5.906in (15cm), and 9.843in (25cm)) and "caught" the ball with the fan. These starting heights were measured from the bottom of the ball.

The aim of this research project is to develop a procedure to control the descent of a ball from images and evaluate the capabilities of camera-based measurements being used in control systems. We will investigate the system's robustness to a wide range of inputs, and will evaluate system robustness by analyzing the percent overshoot after collecting the data.

The goal is to have a controlled descent, with the object ending at a specified ending height – 6 inches from the bottom of the original tube. The variables are: starting height, overshoot, rise time, and ending height. The team sees this project as reasonable in terms of scope, as the materials required are able to be provided by the instructional team. Successful completion of the lab will inform the researchers if camera measurements can be used to control the descent of larger aerial objects, such as drones.

THEORY

We will model the ping pong ball as a point mass and assume that the only forces acting on it are gravity and thrust from the fan (Figure 1). The force balance equation is:

$$\Sigma F = F_{thrust} - F_{gravity} = ma \rightarrow F_{thrust} - mg = ma \quad (1)$$

To determine the fan voltage necessary such that F_{thrust} is sufficient to keep the ping pong ball at a desired height, fan voltage to steady state height data was taken. This will be discussed further in Methods and Materials, Calibration.

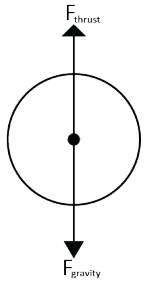

Figure 1: Free body diagram of the ping pong ball.

A Proportional-Integral-Derivative (PID) controller is a feedback compensator controller that uses integration to capture a system's

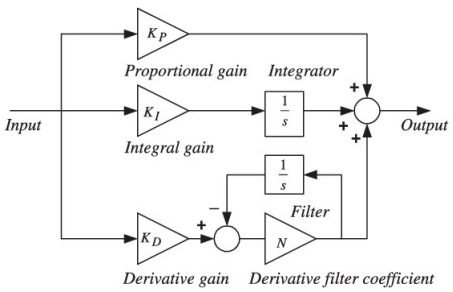

Figure 2: General PID controller [3].

	Rise Time	Overshoot	Settling Time	Steady State Error
$\mathbf{K}_P$	↓	↑	small △	↓
$\mathbf{K}_I$	↓	↑	↑	↓
$\mathbf{K}_D$	small △	↓	↓	no △

Table 1: Summary of PID parameters and their effects on system characteristics.

history and differentiation to anticipate future behavior [3]. The general structure of a PID controller is pictured in Figure 2 and the general effects of changing controller parameters K_P, K_I, and K_D are summarized in Table 1. In our experiment, we use a PID controller to control the height of a ping pong ball, with the ball's position measured as the ball's center.

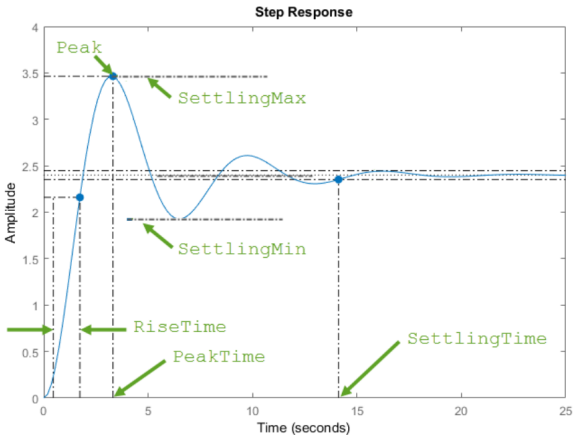

Figure 3: General step response characteristics of a control system [5].

We will look at various characteristics of the system response, pictured in Figure 3, to evaluate the PID's accuracy and robustness and to see how the efficacy of the controller changes as initial drop height is varied. Rise time is the time it takes for the response to increase from 10% to 90% of the steady state value. We will use rise time to evaluate controller reaction time. A system's settling time describes how long it takes for the error between response and steady state value to fall within 2% of steady state. The settling min and max are the minimum and maximum values, respectively, the system reaches once the response has risen. Percent overshoot and undershoot are how much the system output exceeds or falls below, respectively, the steady state value. The overshoot will tell us how accurately the controller can achieve a desired end height. Peak is the max of the absolute value of the response, and peak time is the time at which the peak occurs [5].

In evaluating the experimental results, uncertainty was an important factor for us to take into account. In order to take uncertainty from multiple variables into account, we used Gauss' method for uncertainty propagation:

$$u_a = \sqrt{(\frac{\partial a}{\partial x}u_x)^2 + ... + (\frac{\partial a}{\partial z}u_z)^2} \quad (2)$$

where a is the variable of interest, and x, ..., z are measured with independent, random uncertainties u_x, ..., u_z [4]. A key assumption of Gauss's formula is that the left and right sides are linearly related and, for non-linear terms, the uncertainty is small. This assumption will be considered when Gauss's equation is used in the discussion section.

Based on this model, we expect to be able to command the necessary thrust to keep the ping pong ball aloft at a range of desired heights dependent on the fan capabilities. However, as we increase the initial drop height of the ball, the initial velocity with which the ball enters the camera frame will increase so the controller will either have to react more quickly or will experience more significant overshoot. We expect to see lower rise times, peak times, and settling mins, and increased overshoot, settling times, peaks, and settling maxes as we increase drop height. Additionally, we do not expect to see any undershoot, since we expect that the ball's position will oscillate before settling at our desired input height. Overall, we suspect that the controller performance will decline with increased initial height.

METHODS AND MATERIALS

Overview:

In this experiment, a PID controller is used to control the vertical location of a ball within a tube. The actuator is a fan at the base of the tube, and the sensor is a camera facing the side of the tube. In consideration of real world applications, such as a drone landing, or a rocket propulsive landing, it is necessary to delicately land the ball, and ensure that our control system does not induce an overshoot that causes the ball to crash at the limit. Therefore, this strategy would need to have a low-overshoot criteria, and short response time being a secondary goal. Furthermore, if our system consistently has an overshoot, it is possible to develop statistics to make sure that the ball does not crash because of this, within a certain level of confidence.

Physical Setup:

Materials:

1. Provided fan-tube setup
2. NI Power Supply
3. Basler acA2040-55uc video camera and mount
4. PETG clear tube (2" OD x 1-3/4" ID x 3' length)
5. 3D printed tube clamp
6. 4 x nuts and bolts for clamp
7. 36"x48" white cardboard background
8. Standard ping pong ball, painted black

Figure 4: Camera setup.

The team used the camera and ball-in-tube hardware setup. The camera image acquisition and ball detection were implemented using native functions in LabVIEW. The controller system, which is discussed more in detail in the next section, was then also implemented in LabVIEW. The camera was set up so that it was pointing towards the ball-in-tube setup; the tube was in view, but the ball before being dropped was not, which implied that the ball entered the camera's frame with an initial velocity. The camera was secured to the table using a clamp, as shown in Figure 4.

Figure 5: Hardware setup with extra tube extension.

A 3ft long tube was attached on top of the tube of the test apparatus in order to extend the available area from which to drop the ball (Figure 5. These tubes were chosen to have the same inner diameters. Holes were drilled into the sides of the tube at 1.969in (5cm) increments to allow airflow and for the ball to be dropped at user-selected heights. These holes were drilled using a mill in the Etcheverry Machine Shop, the 1.969in increments were measured by the mill's digital readout.

This additional tube was attached to the original ball-in-tube setup using a custom designed clamp seen in Figure 6, which was CAD modeled in SolidWorks and 3-D printed. The ball was colored black, and the entire test apparatus was placed in front of a white backdrop in order for the imaging system to more easily identify the ball in the tube.

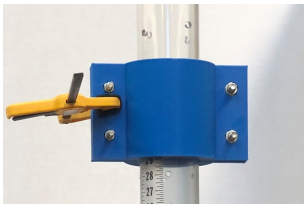

Figure 6: Mounting method for attaching the tube extension.

LabVIEW Implementation:

The LabVIEW VI employed for the experiments mainly revolves around vision acquisition and PID control. First, LabVIEW interfaces with the Basler camera via the Vision Acquisition block. This block outputs video data which is then read by the Vision Assistant block to locate the ball. Within the Vision Assistant, calibration for the camera was performed in order to map the pixels of the video into spatial dimensions (details in "Calibration" section). Vision Assistant also has available the function "Circles Calibrate," which is used for ball tracking. In summary, Vision Assistant inputs video data from Vision Acquisition, and outputs packaged data called "Circles Calibrate."

From "Circles Calibrate," it is necessary to extract ball height, which is the data necessary for the experiment. So, the VI performs multiple "unbundles," which essentially splits up the packaged data until the y position data is revealed as a single numeric array in inches. The y position is subtracted from 6, which is the reference height (6in) to obtain the error. The error array is then plugged into the PID block, along with selected gains ($K_P = 0.3401$, $K_I = 0$, $K_D = 0$). K_P is driven by an open loop gain, which was found from a fan voltage to ball height calibration (details in "Calibration" section). K_I and K_D did not immediately provide much assistance in the ball descent, although further testing may have led to better tuned gains.

The PID block then gives a value which is to be the voltage input. However, it is first negated, added to 7.26 (based on the fan-height calibration for 6 inches reference height, details in "Calibration" section), and saturated to the available fan voltage range using "In Range and Coerce." Finally, this data is bundled with two zeros for Channels 1-3 on the power supply, and fed into the Power Express block, as per the required input for this block. In the LabVIEW

controller (Appendix, Figure 17), a manual voltage is shown to be inputted into the Power Express block, which was utilized only between experiments to reset the ball. Wires are also connected from the y position, and fan input into the "Write to Measurement File," which records the data in time.

Calibration:

Before measurements were taken from the camera, the camera was calibrated using a native function in LabVIEW Vision Assistant called User-Specified Points Calibration. 8 points were mapped from the image to (X,Y) points in real space, and the calibration algorithm then used known mappings to compute pixel to real world mapping for the entire image. This calibration yielded the statistics in Table 2 and the inch to pixel mapping plots can be seen in Figures 7 and 8.

Mean error (in)	Max error (in)	Std. Dev (in)	% Distortion
0.0386577	0.0713074	0.00595923	0.712492

Table 2: Camera calibration statistics.

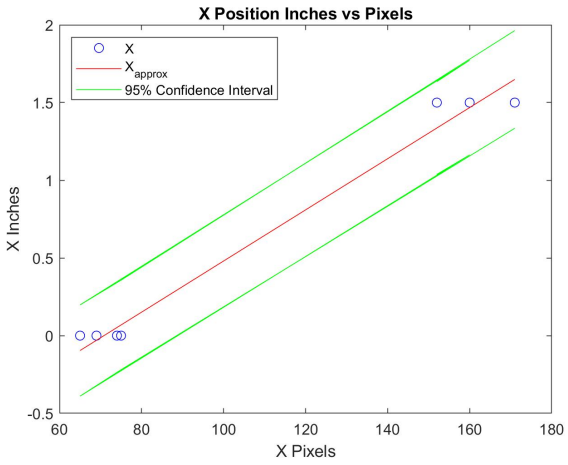

Figure 7: Selected x coordinates paired with corresponding pixel values for dimensional mapping.

Five points were selected along the center axis of the tube in increments of one inch as demarcated by the ruler on tube's outer wall. Also, three points were selected from known vertical heights and located at the edge of the tube horizontally in order to properly calibrate the camera. From this data, our group also computed custom calibration plots in order to calculate confidence intervals and uncertainty. The 95% confidence interval is ± 0.3255 inches, with computed uncertainty of ± 0.0899 inches. Since our sample size was less than 30, we used the student's t-distribution to calculate uncertainty values from the error, rather than the z-distribution.

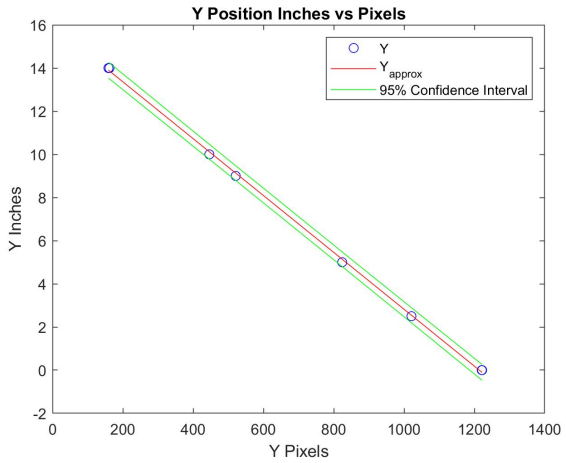

Figure 8: Selected y coordinates paired with corresponding pixel values for dimensional mapping.

$$error = Y - Y_{approx}$$

$$uncertainty = \pm t_{0.025,\nu} \frac{S_x}{\sqrt{\nu}}$$

Then, before starting to tune the gains on the controller, fan voltages were calibrated to steady state hovering heights of the ball. This was done by powering the fan with the power supply using an increasing series of voltages and measuring the steady state height for each. From this data, pictured in Figure 9, an desired steady state height was selected of 6 inches, and the corresponding calculated proportional open loop gain was 7.26 V. A confidence interval and uncertainty were calculated for this calibration using the aforementioned method above. The 95% confidence interval is ± 1.0095 inches, and corresponding uncertainty is ± 0.2726 inches.

The two main sources of uncertainty that were taken into account were the uncertainty from the camera and uncertainty from the fan. Figure 10 shows a diagram of how uncertainty affects the system, and propagated throughout. We can see that the desired height from the controller is skewed by uncertainty of the fan ("System input" to "System output"). Also, the ball height measurements are directly affected by the camera uncertainty ("System output to "Measured output").

Overall, the actual height, "System Output," has a combined "closed loop" uncertainty from both the fan and camera. This resulting uncertainty of the ball height was calculated from the net effect of both of these sources of uncertainty by using Gauss' Propagation of Uncertainty. This method is valid because the uncertainties of the fan and the camera are independent and random.

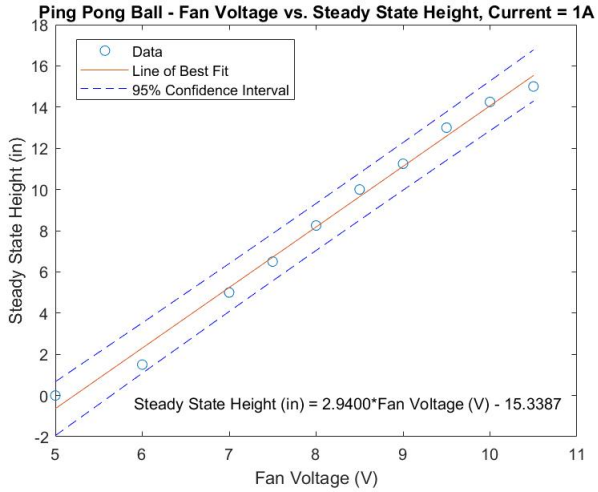

Figure 9: Steady state height of ball at various fan voltages, with current constant at 1A.

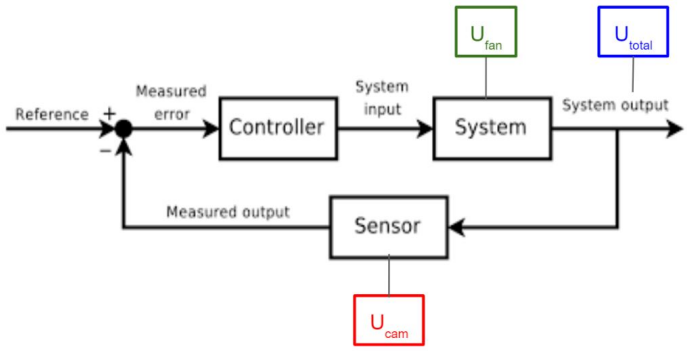

$$U_{cam} = 0.0899\ in$$
$$y_{measured} = y_{actual} \pm 0.0899\ in$$

$$U_{fan} = 0.2726\ in$$
$$y_{actual} = y_{controller} \pm 0.2726\ in$$

$$Gauss'\ Propagation\ of\ Uncertainty$$
$$U_{total} = \sqrt{U_{cam}^2 + U_{fan}^2} = 0.2870\ in$$
$$y_{actual} = y_{ideal} \pm 0.2870\ in$$

Figure 10: Uncertainty Propagation Through System, Fan Voltage and Camera Calibration.

Experiment Procedure and Data Collection:

The main objective of this lab is to effectively characterize the performance and robustness of the controller for the ball descent. To this end, the following parameters will be measured for various drop heights: Rise time, settling time, and overshoot. To obtain these parameters, position, time, and fan voltage data were collected for each drop test. 15 measurements were collected for each of three heights - 1.969in, 5.906in, and 9.843in above the bottom tube.

For each experiment, the ball is initially set at one of the heights mentioned above. To fix it in place, a small pin is inserted into the corresponding hole in the top tube for that height, and the ball rests on top of the pin. This process is repeated to ensure consistency in measurement procedure. The LabVIEW VI is started, and the pin is removed. The pin removal process was implemented to ensure the balls are consistently falling from the same height. The ball then descends until it has entered the bottom tube, and appears in the camera frame, at which point the Vision Assistant recognizes the ball and assigns its height. Here, the controller can finally begin to regulate the fan voltage and attempt to control the ball's height. After a few seconds pass and the ball has descended, the program is shut off and the data is recorded as an .xls file, to be processed later.

RESULTS

The position vs time and fan voltage vs time data for all runs are plotted and pictured in Figures 19 - 25 in the Appendix, but summaries of the response characteristics for each drop height are given in Tables 3 - 5. These characteristics were generated by using MATLAB's stepinfo( ) function on the collected datapoints, ignoring outliers which are discussed further in the Discussion section. The team collected at least 10 data points for each drop to ensure results were representative.

Run	RiseTime (s)	SettlingTime (s)	SettlingMin (in)	SettlingMax (in)	Overshoot (%)	Undershoot (%)	Peak (in)	PeakTime (s)
1	0.287	NaN	5.900	9.301	25.977	0	9.301	0.457
2	0.052	NaN	5.324	9.301	28.037	0	9.301	0.124
3	0.060	NaN	5.991	9.301	25.843	0	9.301	0.380
4	0.068	NaN	4.977	9.301	19.539	0	9.301	0.265
5	0.061	NaN	4.881	9.301	21.011	0	9.301	0.120
6	0.069	NaN	4.919	9.301	21.809	0	9.301	0.150
7	0.153	NaN	4.841	9.301	19.276	0	9.301	0.316
8	0.084	NaN	5.453	9.301	18.761	0	9.301	0.162
9	0.074	NaN	4.796	9.301	19.046	0	9.301	0.148
10	0.069	NaN	5.043	9.301	22.713	0	9.301	0.147
11	0.077	NaN	5.002	9.418	23.675	0	9.418	7.642
12	0.101	NaN	4.951	9.301	18.302	0	9.301	0.271
13	0.127	NaN	5.050	9.301	20.391	0	9.301	0.496
14	0.313	NaN	5.130	9.301	21.392	0	9.301	1.267
15	0.197	NaN	4.921	9.301	20.953	0	9.301	0.687
avg	0.120	NaN	5.145	9.309	21.782	0	9.309	0.842

Table 3: Response characteristics for ball drops from 1.969in.

The team expected the controller to guide the ball in a manner similar to that of a traditional control system, shown in Figure 3. However, the controller used was not able to reach a steady-state height,

Run	RiseTime (s)	SettlingTime (s)	SettlingMin (in)	SettlingMax (in)	Overshoot (%)	Undershoot (%)	Peak (in)	PeakTime (s)
1	0.066	NaN	5.334	9.301	22.039	0	9.301	0.389
2	0.070	NaN	5.267	9.301	18.664	0	9.301	0.245
3	0.067	NaN	5.213	9.301	20.614	0	9.301	0.376
4	0.055	NaN	5.006	9.301	19.753	0	9.301	0.108
5	0.060	NaN	5.407	9.301	21.705	0	9.301	0.120
6	0.069	NaN	5.218	9.301	15.977	0	9.301	0.307
7	0.086	NaN	4.765	9.301	18.069	0	9.301	0.160
8	0.743	NaN	5.221	9.301	20.468	0	9.301	1.075
9	0.080	NaN	5.251	9.301	17.479	0	9.301	0.147
10	0.225	NaN	4.987	9.301	12.470	0	9.301	0.638
avg	0.152	NaN	5.167	9.301	18.724	0	9.301	0.357

Table 4: Response characteristics for ball drops from 5.906in.

Run	RiseTime (s)	SettlingTime (s)	SettlingMin (in)	SettlingMax (in)	Overshoot (%)	Undershoot (%)	Peak (in)	PeakTime (s)
1	0.261	NaN	5.386	9.301	19.490	0	9.301	0.491
2	0.135	NaN	5.940	9.301	17.546	0	9.301	0.248
3	0.065	NaN	5.215	9.301	17.180	0	9.301	0.253
4	0.106	NaN	4.921	9.301	15.515	0	9.301	0.185
5	0.055	NaN	5.467	9.301	21.186	0	9.301	0
6	0.210	NaN	4.855	9.301	19.244	0	9.301	0.459
7	0.075	NaN	4.855	9.301	15.771	0	9.301	0.274
8	0.076	NaN	5.406	9.301	19.643	0	9.301	0.156
9	0.083	NaN	5.067	9.301	20.359	0	9.301	0.488
10	0.078	NaN	5.164	9.301	18.094	0	9.301	0.344
avg	0.114	NaN	5.228	9.301	18.413	0	9.301	0.290

Table 5: Response characteristics for ball drops from 9.843in.

and the ball height was skewed by invalid ball identification measurements. A few representative plots can be seen in Figure 11.

The team chose to analyze the collected data using: rise time, settling time, settling minimum, settling maximum, overshoot, undershoot, peak, and peak time. The average values for these characteristics are summarized in Table 6. As summarized at the bottom of Table 6, the trends we expected to see vs the actual trends we saw did not align much at all. The rise time for the ball dropped from the three heights sorted from smallest to largest, is 0.120s, 0.152s, and 0.114s, and did not follow a consistent trend. Because our controller performed poorly, the ball was never able to settle at a steady state height. As a result, we had no settling time data. The settling minimum for that range increased from 5.145in to 5.167in to 5.228in. This is the opposite of what we expected. The average settling maximum and peak stayed relatively constant, changing from 9.309in to 9.301in and 9.301in. We expected settling max and peak to increase, but these values were greatly impacted by the outliers in our data since the outlier was larger than our other data values. The outlier essentially masked any other max or peak points we might otherwise have seen. The average overshoot percentage over that same period decreased as follows: 21.782%, 18.724%, 18.413%, which again was the opposite of what we had expected. Because our system was not overdamped, we did not get any undershoot which was as expected. Finally, the peak time varied from 0.842s to 0.357s to 0.290s, respectively, which was as expected.

DropHeight (in)	RiseTime (s)	SettlingTime (s)	SettlingMin (in)	SettlingMax (in)	Overshoot (%)	Undershoot (%)	Peak (in)	PeakTime (s)
1.969	0.120	NaN	5.145	9.309	21.782	0	9.309	0.842
5.906	0.152	NaN	5.167	9.301	18.724	0	9.301	0.357
9.843	0.114	NaN	5.228	9.301	18.413	0	9.301	0.290
expected	↓	↑	↓	↑	↑	↓	↑	↓
actual	NA	NA	↑	↓	↓	NA	↓	↓

Table 6: Average response characteristics at each drop height summarized.

The collected data ultimately differed greatly from the theoretical model. We saw that as the drop height was increased from 1.969in to 9.843in, the average rise time across all drop heights increased from 1.066s to 3.353s. Following the increase in drop height, the average overshoot percentage across all drop heights fell from 9.264% to 3.580%. Based on the theoretical model, the team expected the overshoot percentage to increase as the drop height increased, but that was not the case, so the team determined that the results were greatly skewed by the outliers.

DISCUSSION

Overall, the controller was able to use images from the Basler camera to control the fan voltage and, subsequently, the location of the ball. However, there were issues with the calibration and opportunities to improve the testing for the future.

One of the issues that may have contributed to poor performance of the controller is that the imaging system detected a circle at 9.301in consistently in all data runs regardless of the actual position of the ball. This position value appeared in instances that did not make logical sense, as the position values both before and after were consistently different than the 9.301in value. This led the team to deduce that there was a mistake in the imaging system setup which caused detection of a "ghost" circle at 9.301in. Since these false circles were so far from our desired height, the controller would command 0V to the fan in order to compensate. This phenomenon is highlighted in Figure 11 and can be seen in all of our plots in the Appendix, Figures 19 - 25. The team believes that this behavior greatly skewed our experimental results and our ability to accurately evaluate our controller's abilities.

Additionally, only the proportional gain, K_P, was ever tuned for the controller, and the integral gain, K_I, and derivative gain, K_D, were left at 0 during the length of the experiment due to lack of time. If the gains had been tuned over more iterations prior to collecting data for the experiment, the controller may have showed better resulting performance with reduced overshoot and decreased rise time.

The resulting steady state height of the majority of the experiment runs does not fall within the uncertainty bounds of ± 0.2870 inches previously established by the Gauss' Propagation of Uncertainty calculation. Though the plots exhibit that the controller is able to stabilize the descent of the ball and cause it to oscillate around the desired steady state height of 6 inches, the controller is unable to

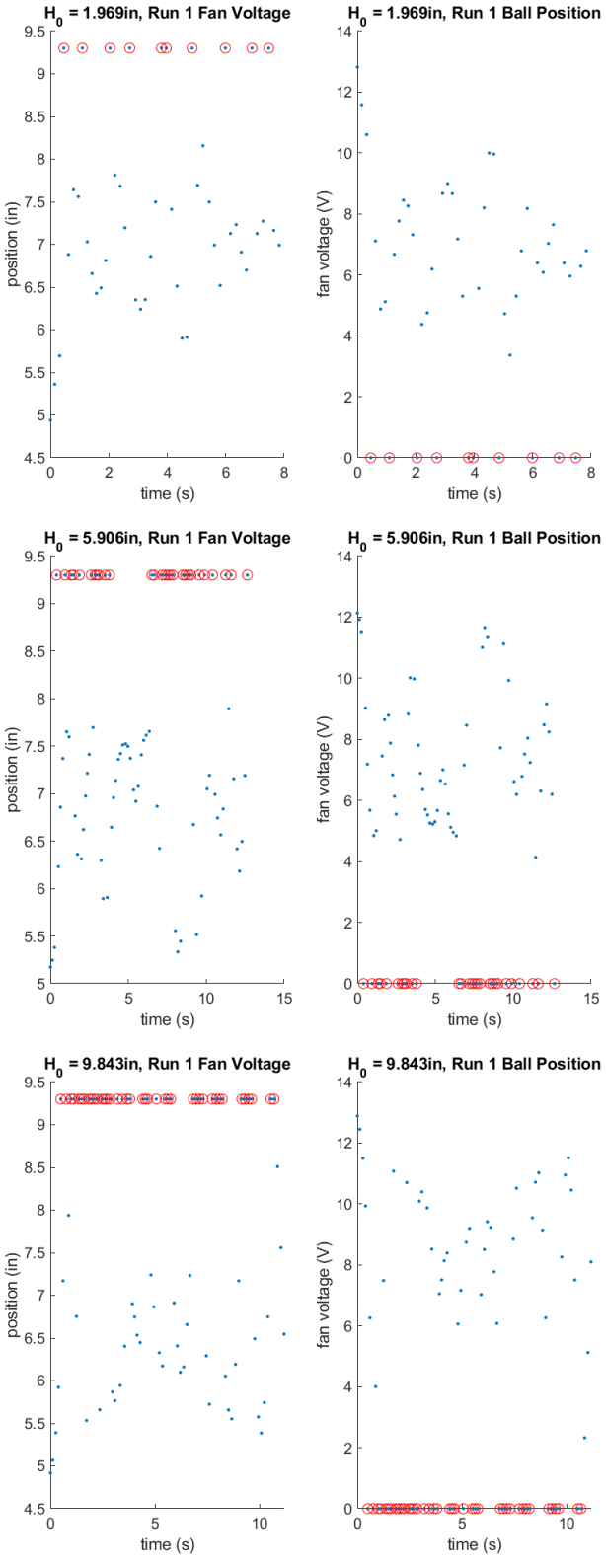

Figure 11: A few samples highlighting the false data points are shown here with the points corresponding to the false circle at 9.301in circled in red.

overcome uncertainty in the system and command the steady state height within the predicted uncertainty bounds.

In the future, the team would spend more time on creating a image-detection mechanism that is more accurate. The image-detection method that was used malfunctioned more than was expected, as shown by the amount of "ghost" circles in Figure 11. The team would also invest in a more stable camera setup, as the setup used was merely a clamp secured to the camera's wire on a desktop. There may have been movements in the camera setup that contributed to the inaccuracy of the ball-detection mechanism.

CONCLUSION

The goal of this experiment was to understand if an external camera could control the descent of a ping-pong ball, with initial downward velocity, connected to a fan. The tests revealed that position control using an image-based input can be accomplished in real time. Additionally, the camera and fan voltage calibration uncertainties contribute significantly to controller performance, and therefore the tuned controller must overcome uncertainties from the camera and fan in order to be robust enough to be used to control the vertical location of a drone in the real world. In a real life application of this technology to land an object at or near the ground, it would be important for the settling min to be at or above the desired height, otherwise the object would crash into the ground. Future researchers are recommended to minimize oscillations, fine tune the controller, and debug the ball tracking system.

References

[1] Ayars, Eric. "PID Ping-Pong Ball Levitation." Physics 427, CSU Chico, 4 Sept. 2018.

[2] Goddings, James. "Position Control of a Ping-Pong Ball," London South Bank University. Nov. 22, 2015.

[3] Messner, Bill, and Dawn Tilbury. "Introduction: PID Controller Design." Control Tutorials for MATLAB and Simulink - Introduction: PID Controller Design, University of Michigan, CMU, NSF, MathWorks,

[4] Palmer, M. "Propagation of Uncertainty through Mathematical Operations." MIT Fluids Modules, Massachusetts Institute of Technology.

[5] "stepinfo", The MathWorks Inc.

[6] W. Kexin, S. Michael, O. Ziwei, "The experiment 'Ball-in-tube' with Fuzzy-PID Controller Based on Dspace", 2007 IEEE International Conference on Systems, Man and Cybernetics, 2007.

APPENDIX

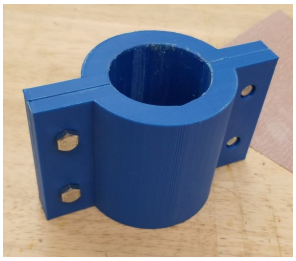

Figure 12: Pipe mount used to attach extra tube to the provided setup

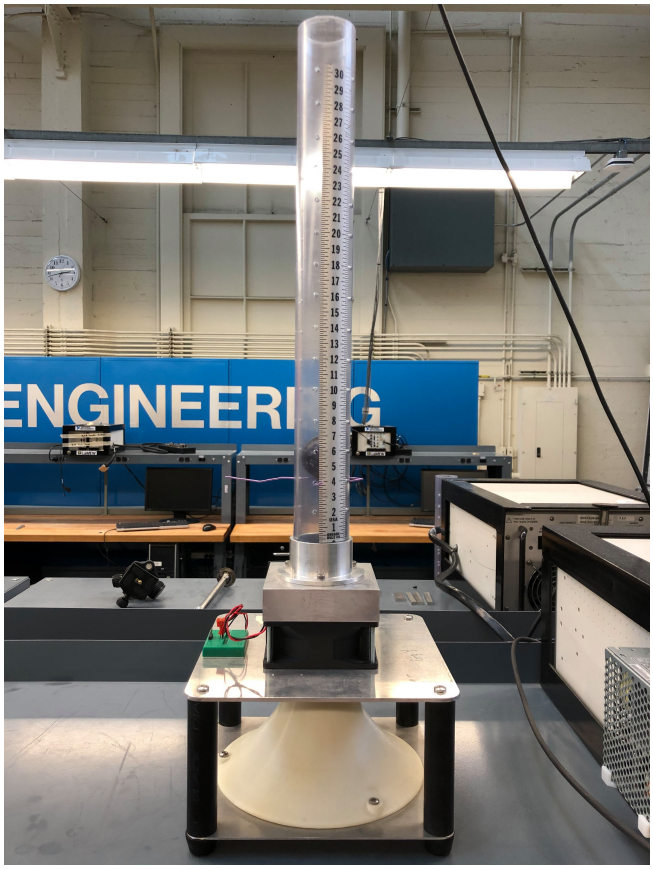

Figure 13: Original ball in tube experiment setup.

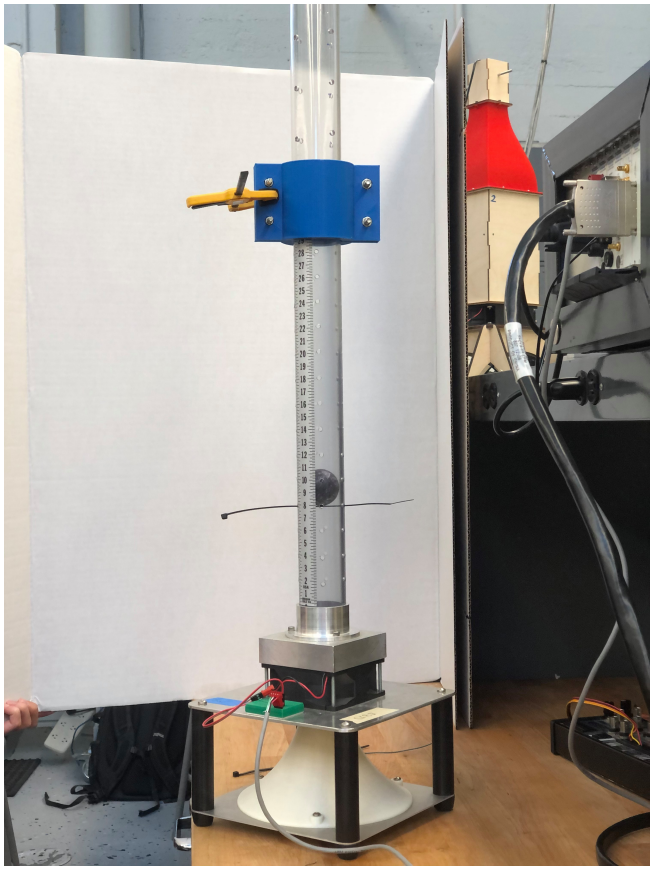

Figure 14: Modified experimental setup with extra tube.

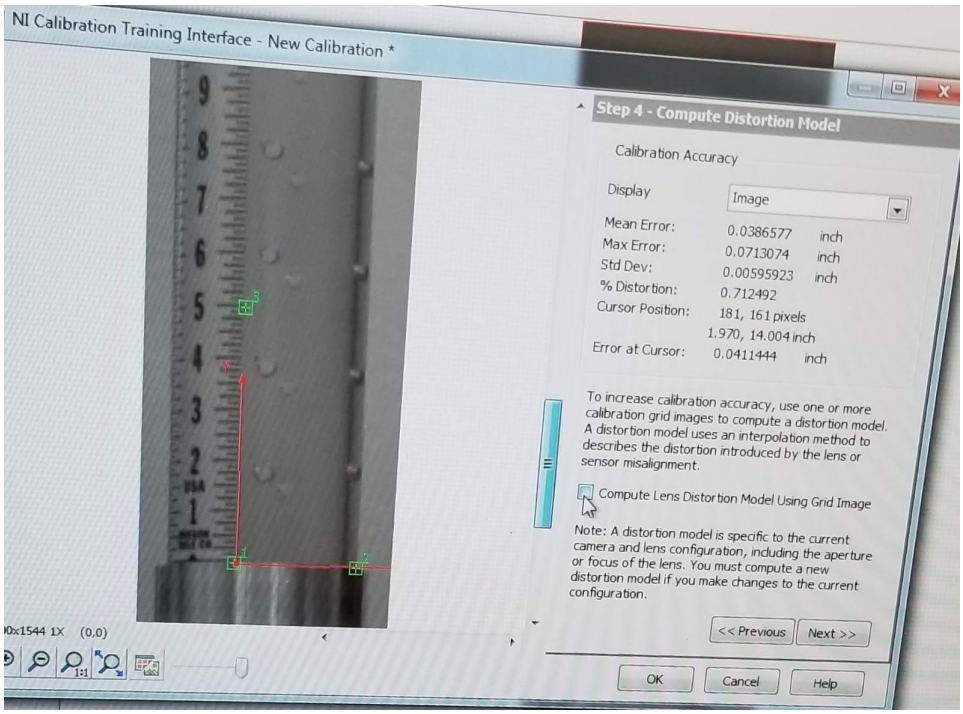

Figure 15: Final calibration of camera.

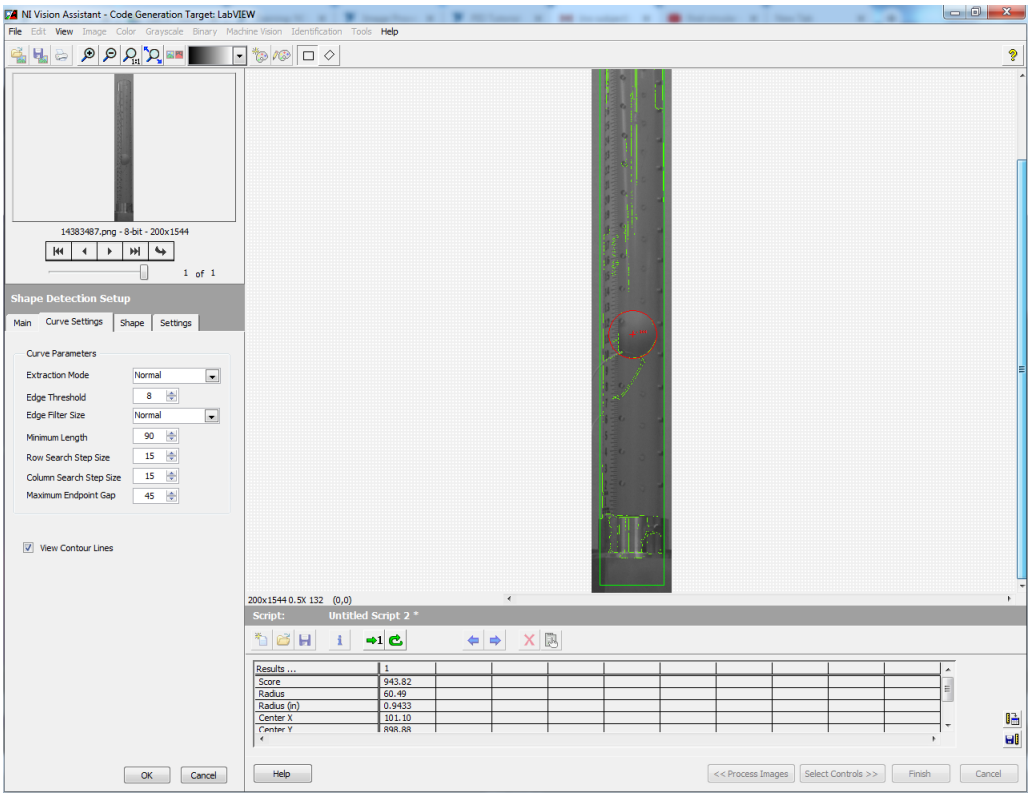

Figure 16: LabVIEW's vision assistant shape detection tool used to find the location of the ping pong ball.

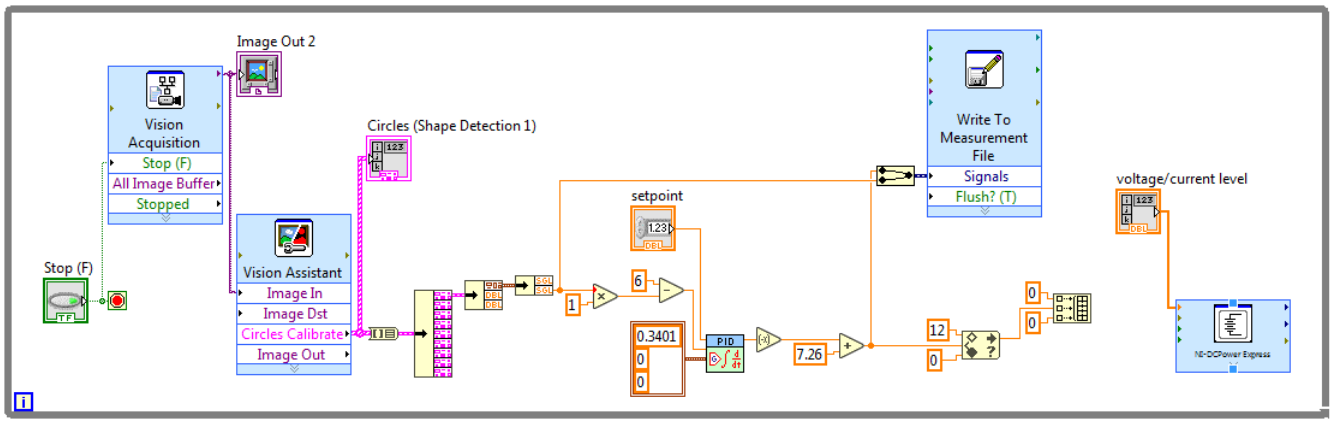

Figure 17: LabVIEW VI controller Block Diagram.

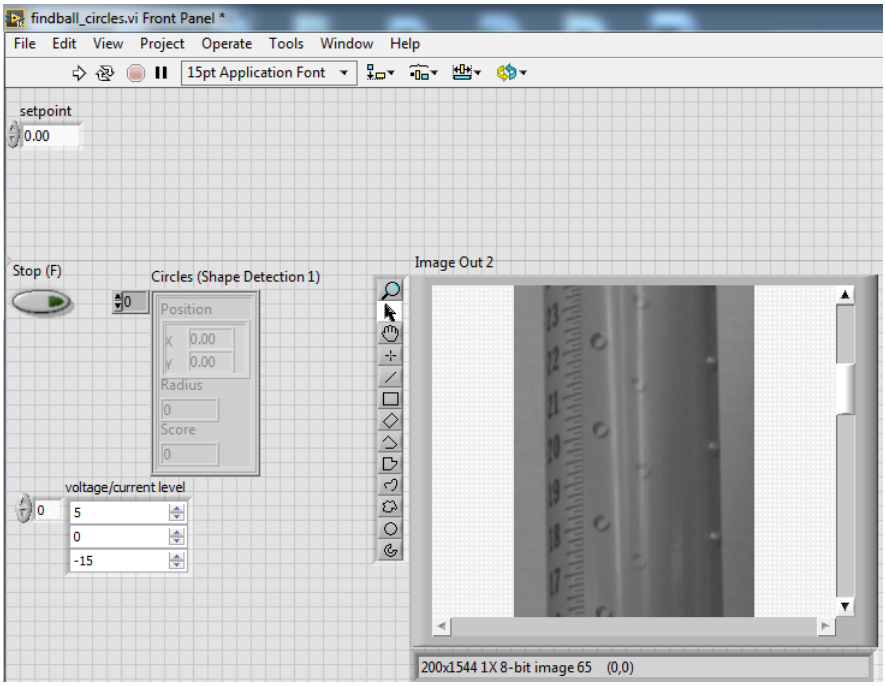

Figure 18: LabVIEW VI controller Front Panel.

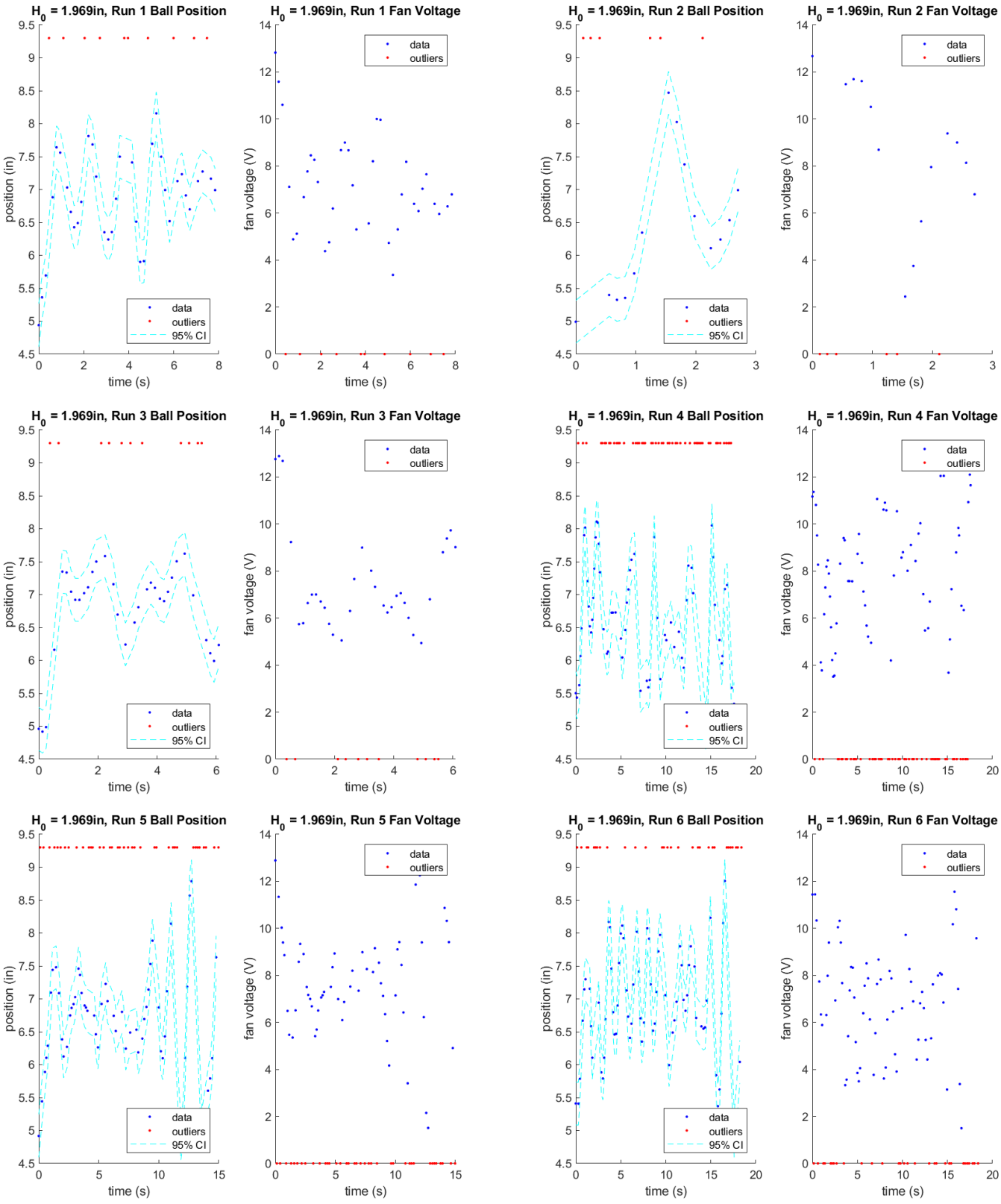

Figure 19: Position and fan voltage plots for initial drop height of 1.969in, runs 1-6.

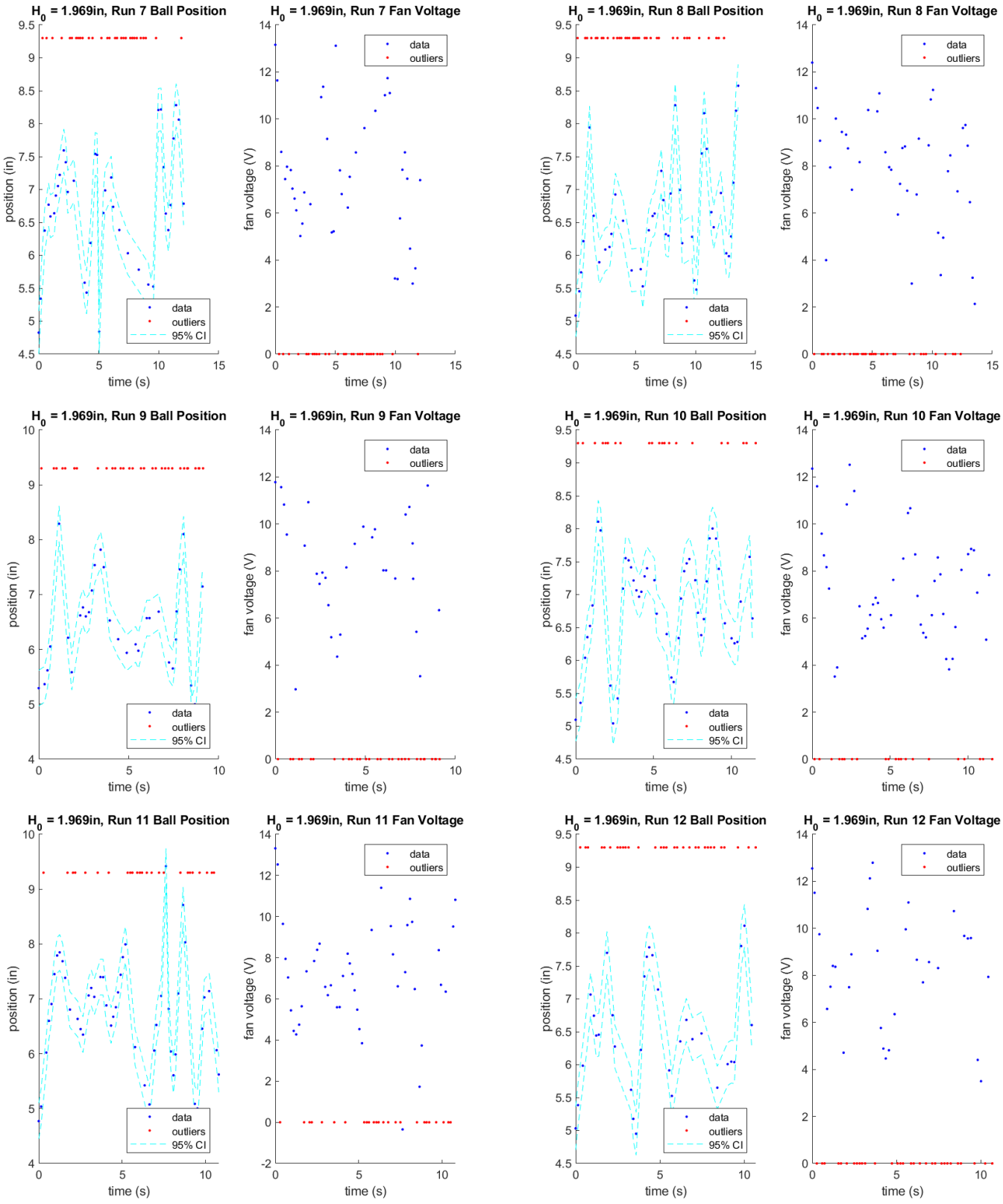

Figure 20: Position and fan voltage plots for initial drop height of 1.969in, runs 7-12.

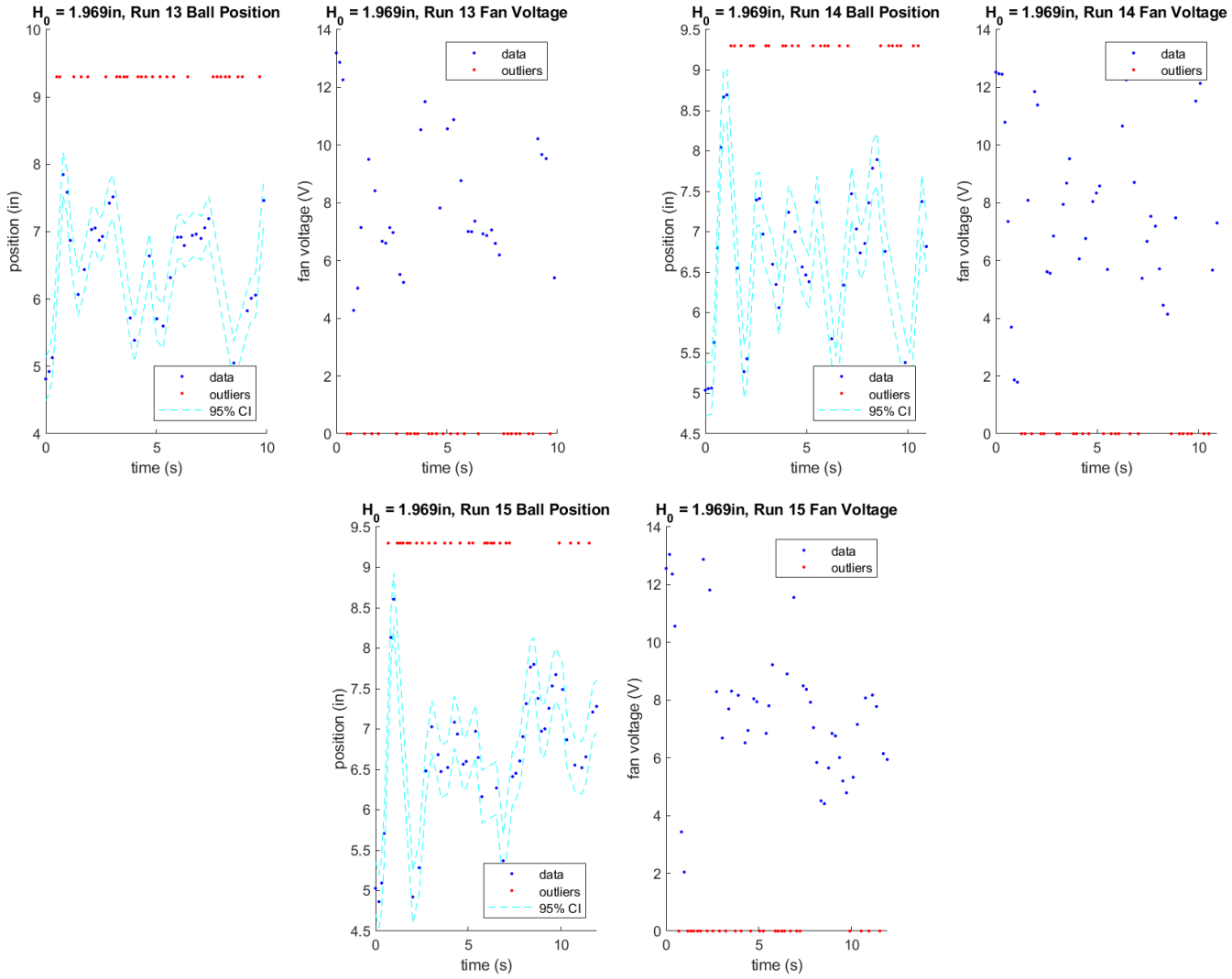

Figure 21: Position and fan voltage plots for initial drop height of 1.969in, runs 13-15.

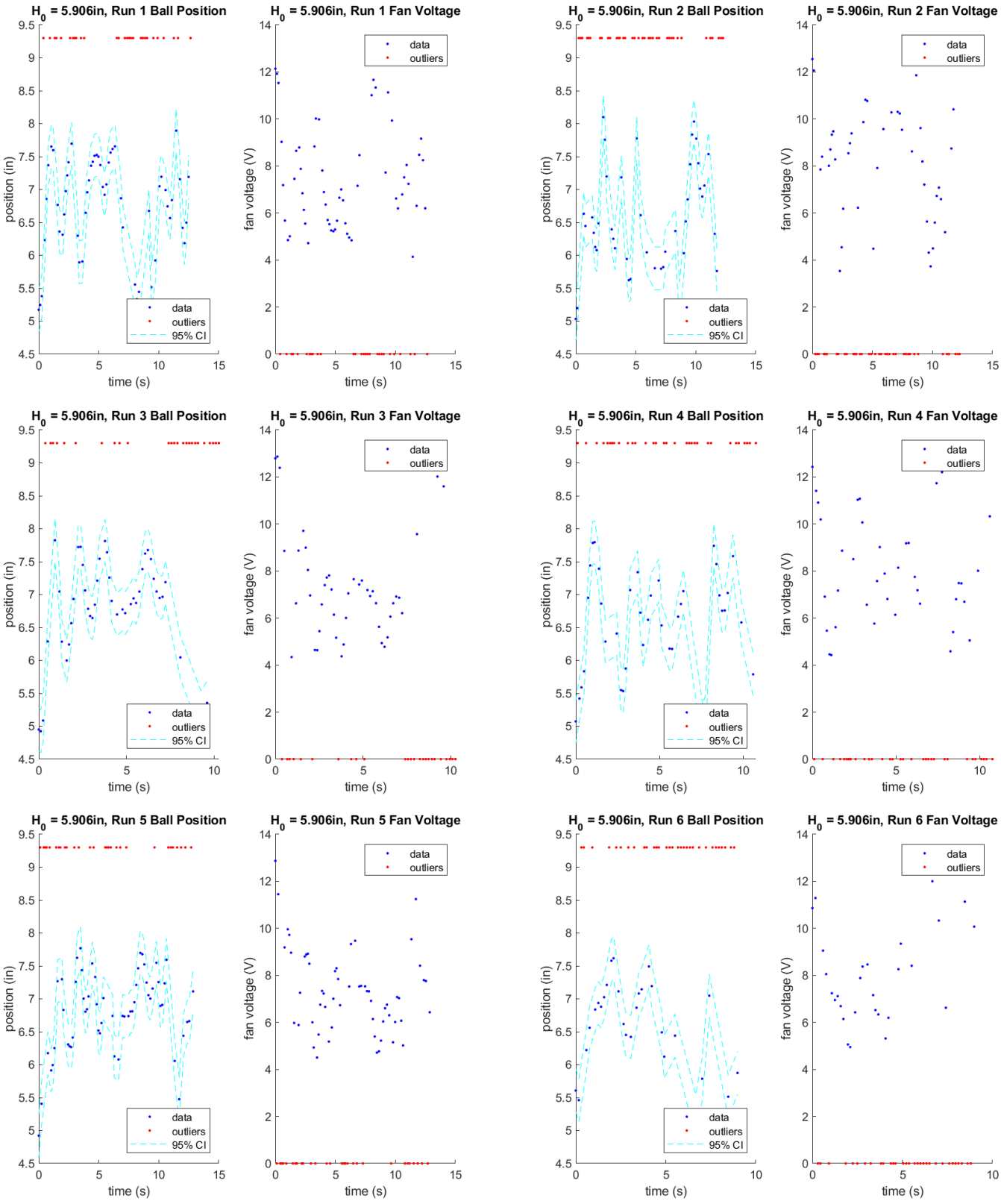

Figure 22: Position and fan voltage plots for initial drop height of 5.906in, runs 1-6.

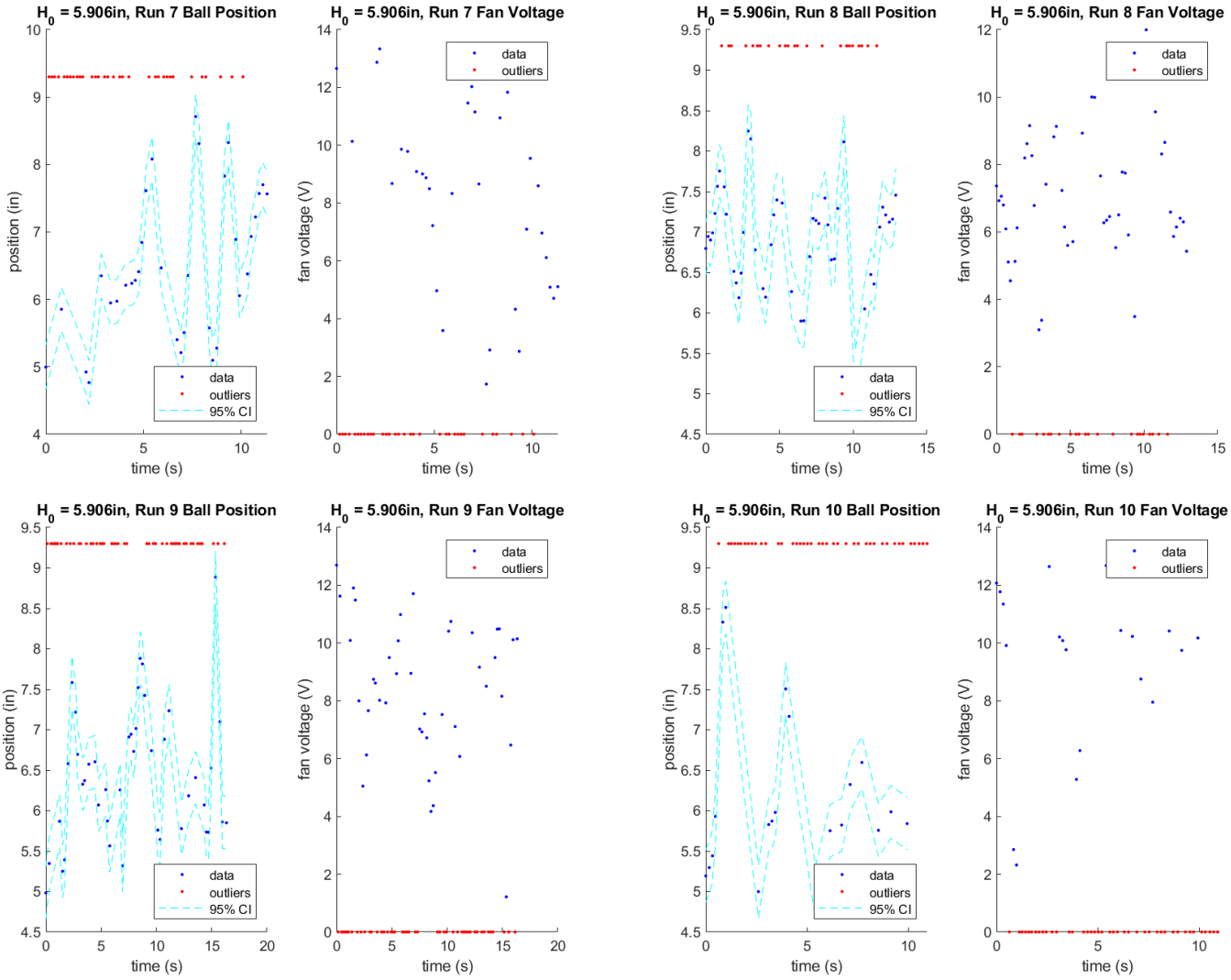

Figure 23: Position and fan voltage plots for initial drop height of 5.906in, runs 7-10.

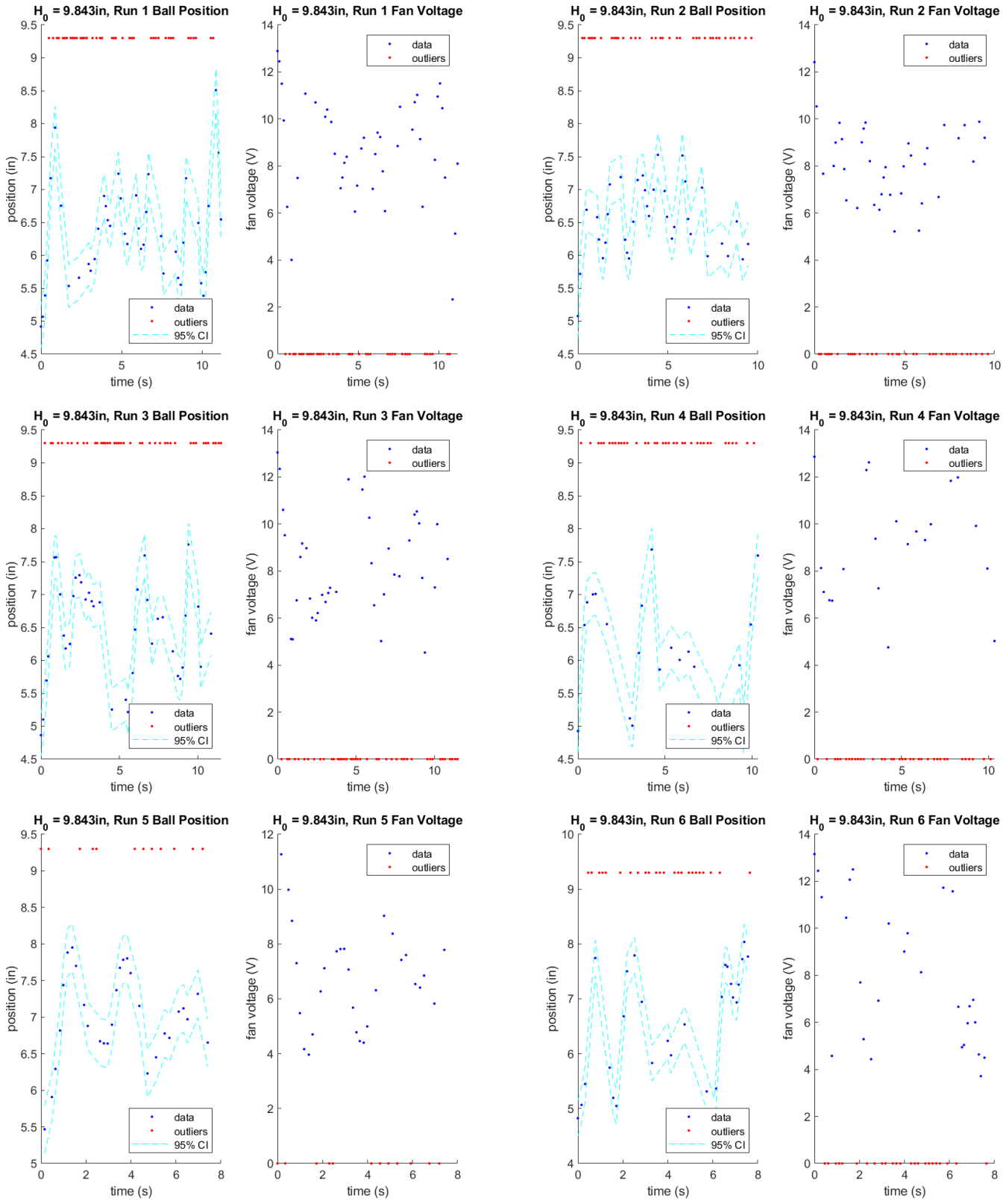

Figure 24: Position and fan voltage plots for initial drop height of 9.843in, runs 1-6.

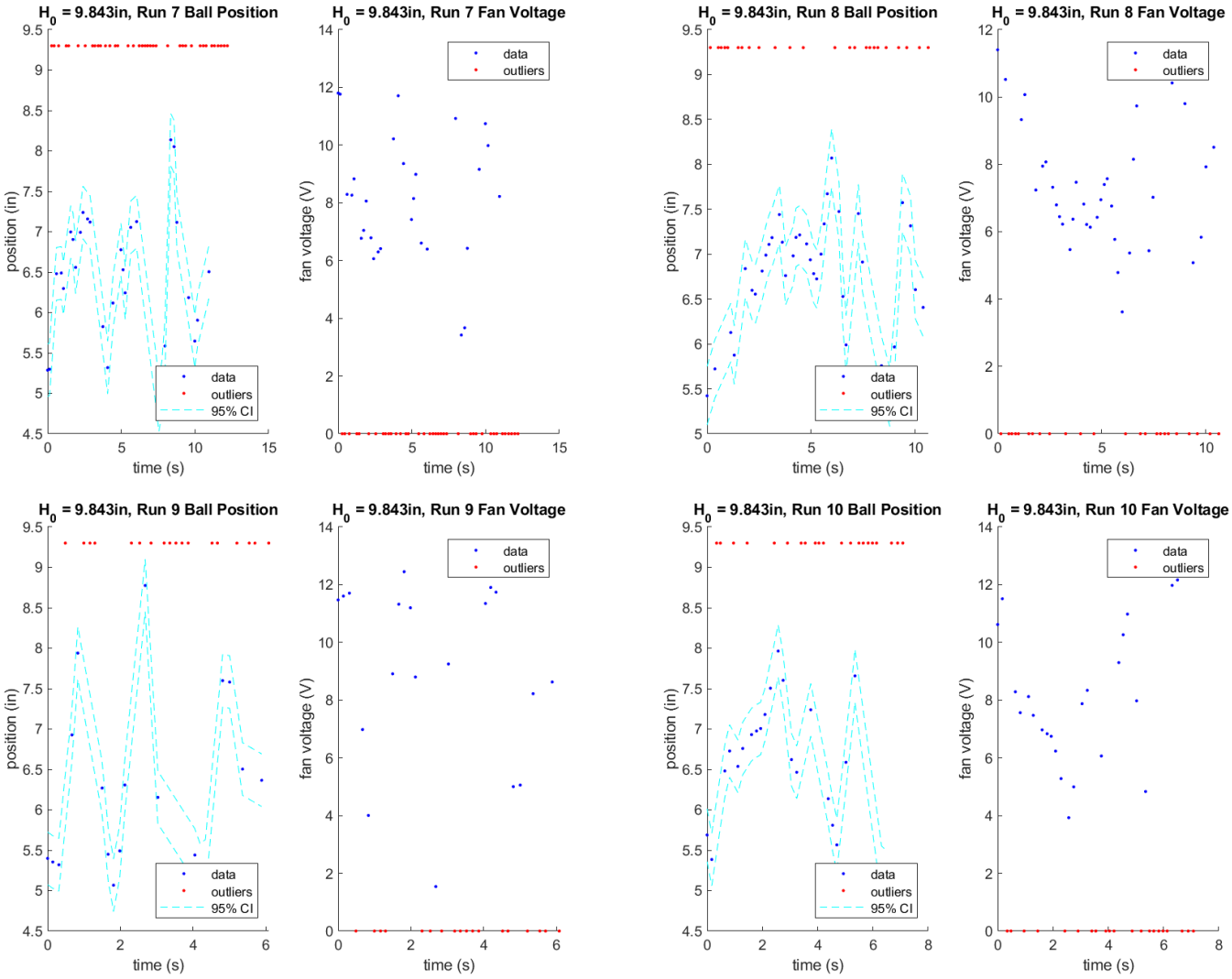

Figure 25: Position and fan voltage plots for initial drop height of 25cm, runs 7-10.